International Journal of Electrospun Nanofibers and Applications,
Vol.1 No. 2 (July-December, 2015)
ISSN : 0973-628X

Effects of PVP Concentration on Structure of Electrospun Titanium Dioxide (TiO_2) Nanofibers

Wirat Jarernboon, Vittaya Amornkitbamrung Ekaphan Swatsitang, Thanusit Burinprakhon, & Santi Maensiri*

Integrated Nanotechnology Research Center (INRC), Khon Kaen University, and Solid State Laboratory, Department of Physics, Faculty of Science, Khon Kaen University, Khon Kaen, 40002, Thailand

Abstract: *Titanium dioxide (TiO_2) nanofibers were fabricated by electrospinning technique using the titanium(diisoproproxide) bis(2,4-pentanedionate) 75 wt% in 2-propanol solution in the presence of polyvinylpyrrolidone (PVP) as a polymer source. The as-spun TiO_2/PVP composite nanofibers (with 7, 10, and 15 wt.% PVP) were characterized by TG-DTA to determine the thermal decomposition and crystallization temperature. TiO_2 nanofibers with diameters of 60-100 nm were obtained from calcinations of the as-spun TiO_2/PVP composite nanofibers at 500°C in air for 3h. The influence of PVP concentration on the structure of TiO_2 nanofibers were investigated by using X-ray diffraction (XRD) and Raman spectroscopy. The TiO_2 nanofibers were also characterized by using Scanning Electron Microscope (SEM), Energy dispersive X-ray spectroscopy (EDS), and Brunauer-Emmett-Teller (BET). The average diameter of as-spun nanofibers and TiO_2 nanofibers increases whereas the number of beads reduce when the PVP concentration increases. The highest surface area of the nanofibers is 90 m^2/g at the PVP concentration of about 7 wt.%. It was found that PVP noticeably affected the formation of rutile phase of TiO_2 nanofibers. At the same calcination temperature, high concentration of PVP (10 and 15 wt.% PVP) caused the formation of rutile phase.*

Keyword: *Electrospinning; Titanium dioxide; Nanofiber; polyvinylpyrrolidone (PVP); X-ray diffraction; Raman spectroscopy.*

1. INTRODUCTION

In recent years, nanomaterials have attracted great attention due to their unique structure and properties. One-dimensional (1D) nanostructured metal oxides have been particularly of great interest because of their unique properties and potential applications in electronics, photonics and other related areas [1-3]. Nanocrystalline titanium dioxide (TiO_2) is a well-known material and is widely studied for its potential applications in chemical sensors, photoelectrochemical cells, optical filters, and systems with enhanced catalytic activity [4-8]. Various methods have been used to synthesize nanocrystalline TiO_2 in the forms of nanoparticles [9], nanotubes [10], nanowires or rods [11], and nanofibers [12]. Most recently, TiO_2–based nanofibers fabricated by electrospinning have been of great interest due to the wide potential applications of nanofibers [13-21]. Electrospinning represents a simple and convenient method for preparing polymer fibers

* corresponding author: E-mail: *sanmae@kku.ac.th; santimaensiri@gmail.com*

and ceramic fibers with both solid and hollow interiors that are exceptionally long in length, uniform in diameter ranging from tens of nanometers to several micrometers, and diversified in compositions [22-26]. In the preparation of electrospun TiO_2 nanofibers, polyvinylpyrrolidone (PVP) has been successfully used as a polymer source, and gives uniform nanofibers of the resultant TiO_2 [13,14,21]. However, the effects of PVP concentration on the morphology and structure of electrospun TiO_2 nanofibers have not much been reported.

In this study, we investigated the influences of PVP concentration on morphology and structure of TiO_2 nanofibers fabricated by electrospinning. The as-spun and calcined TiO_2/PVP composite nanofibers were characterized using X-ray diffraction (XRD), Raman spectroscopy, and scanning electron microscopy (SEM) equipped with energy dispersive X-ray spectrometer (EDS). The surface area of samples was characterized by Brunauer-Emmett-Teller (BET) surface area measurement.

2. EXPERIMENTAL PROCEDURE

2.1 Preparation of TiO_2 Nanofibers

In this study, titanium(diisoproproxide) bis(2, 4-pentanedionate) 75 wt% in 2-propanol abbreviated TIAA (Acros organics, 99%), polyvinyl pyrrolidone (PVP) (M_n = 1 300 000, Aldrich), acetic acid (BDH, 100%) and ethanol (BDH, 100%) were used as the starting chemicals. The preparation of TiO_2/PVP solution for electrospinning is similar to that reported in our previous study [21]. In a typical procedure, the PVP/ethanol solutions with the PVP concentrations of 7, 9, 10 and 15 wt.% were prepared by dissolving PVP in ethanol. To obtain a solution of TiO_2, 1.5 ml (1.485 g) of TIAA was dissolved in 3 ml acetic acid and 3 ml ethanol. The solution was then dissolved in the prepared PVP/ethanol solution. The mixture was vigorously stirred at room temperature to get a homogeneous polymer solution for electrospinning. The schematic electrospinning setup used for the electrospinning process is shown in Fig. 1. The polymer solution was loaded into a plastic syringe equipped with a 22-gauge needle made of stainless steel. The needle was connected to a high-voltage supply (DEL High Voltage (0-100 kV), DEL Electronics Corp., USA). The voltage for electrospinning was 9.0 kV. The solution was fed at a rate of 0.5 mL/h using a syringe pump (TERUMO Terufusion Syringe pump TE-331, Japan). A piece of flat aluminum foil was placed 15 cm below the tip of the needle, and used to collect the nanofibers. All electrospinning processes were carried out at room temperature.

2.2 Materials Characterization

The as-spun TiO_2/PVP composite nanofibers were subjected to thermogravimetric-differential thermal analysis (TG-DTA) using Pyris Diamond TG/DTA (PerkinElmer Instrument, USA). This was done to determine the temperatures of possible decomposition and crystallization (or phase changes) of the nanofibers. The analyses were performed with a heating rate of 15°C/min in static air up to 1000°C. The nanofibers were calcined at 500°C for 3h in air in box furnace (Lenton Furnaces, UK), using heating and cooling rates of 5 min/°C.

Powder X-ray diffraction (XRD) was used for crystal phase identification and estimation of the crystallite size. The X-ray Diffraction measurements were performed on a Phillips X-ray diffractometer (PW3710 mpd control, The Netherlands) with CuKa radiation ($\lambda = 0.15406$ nm). The fraction of rutile phase in each sample was determined via the generally accepted quantitative method [27]. The volume fractions of anatase and rutile were calculated from the (101) reflection of anatase and the (110) reflection of rutile. The volume fraction of rutile present in the composites after various calcinations were calculated using the following equation [28]:

$$X_R = \left(1 + 0.8\frac{I_A}{I_R}\right)^{-1}$$

where X_R is the volume fraction of rutile, I_A and I_R are the integrated line intensities of the anatase and rutile, respectively.

The Raman spectra were performed at room temperature by using a triple spectrometer (Jobin Yvon/Atago-Bussan T-64000, France) with a liquid nitrogen cooled CCD detector for 800 s, in micro-mode. The Ar^+ laser beam with the excitation λ = 638.2 nm with an output power of 20 mW was focused under 90x microscope objective and the laser spot size was between 1 and 2 mm. Raman spectra were recorded in the 850–50 cm^{-1} range. The spectral resolution was 1 cm^{-1}.

The morphology of the as-spun and calcined TiO_2/PVP composite nanofibers was characterized by SEM (LEO SEM 1450VP, U.K.), which is equipped with energy dispersive X-ray spectrometer (EDS). Measurements of ~100 random fibers taken from SEM micrographs were used to determine average fiber diameter and distribution. The BET surface area of the TiO_2 nanofiber was obtained with nitrogen adsorption in a Micromeritics ASAP 2010 nitrogen adsorption apparatus.

RESULTS AND DISCUSSION

The results of TG and DTA analyses of the as-spun TiO_2/PVP composite nanofibers at different PVP concentrations are shown in Fig. 2. The DTA curve depicted an exothermic peak at ~80°C, which indicates the loss of moisture and trapped solvent (water, ethanol and carbon dioxide). According to the DTA curve, all the samples exhibited two strong endothermic peaks, but they have difference peak positions. The first strong peaks at 348°C (TiO_2/7 wt.% PVP), 341°C (TiO_2/10wt.% PVP) and 340°C (TiO_2/15 wt.% PVP) corresponded to the loss of organic species from the crystals and the decomposition of TIAA along with the degradation of PVP by a dehydration on the polymer side chain, which was confirmed by a dramatic weight loss in TG curve at the corresponding temperature range. The second strong peaks at 479°C (TiO_2/7 wt.% PVP), 459°C (TiO_2/ 10 wt.% PVP) and 451°C (TiO_2/15 wt.% PVP) corresponded to the decomposition of main chain of PVP and the formation of metal oxide anatase phase of TiO_2 [13,21]. In addition, it is seen that 15 wt.% PVP can effectively promote the formation of TiO_2 at lower temperature than the others.

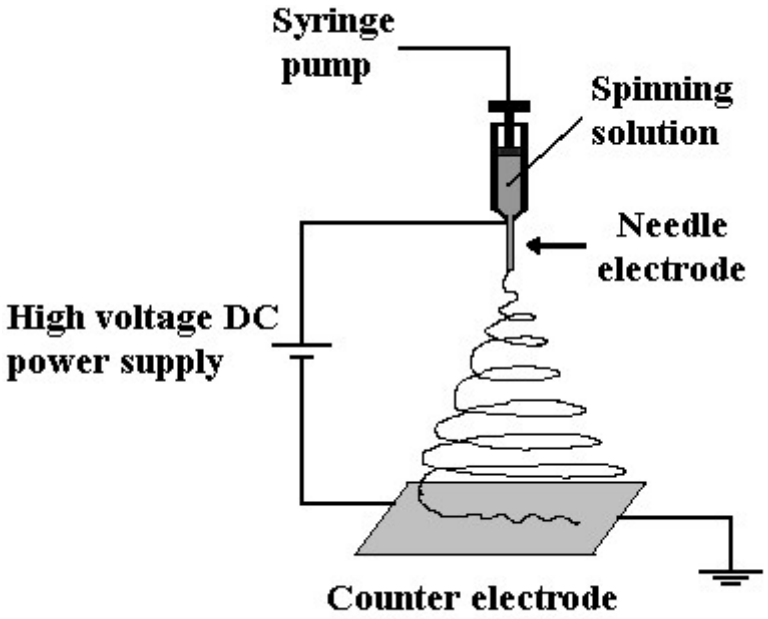

Figure 1: Schematic diagram of electrospinning set up.

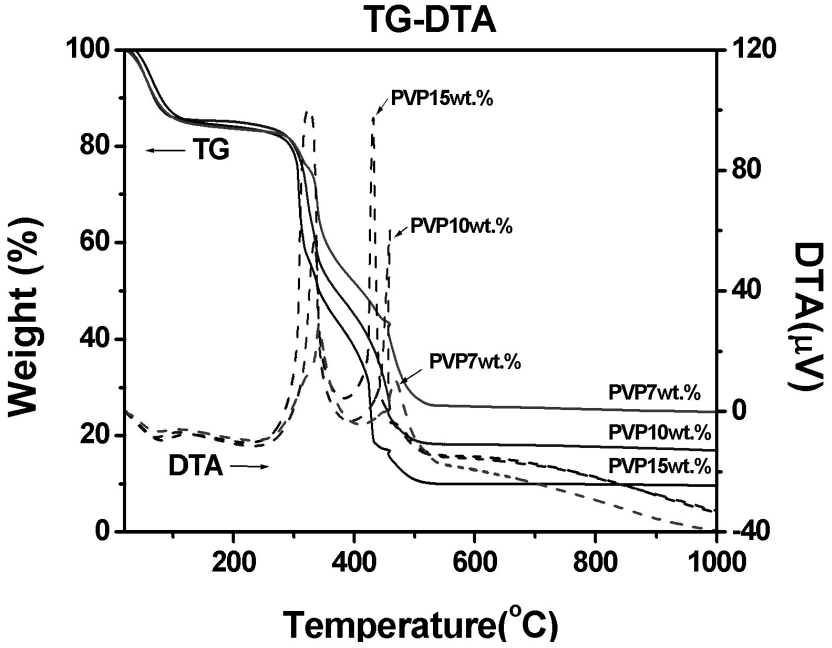

Figure 2: TG-DTA curves of thermal decomposition of the as-spun TiO_2/PVP composite nanofibers at a heating rate of 15°C/min in static air.

Figure 3 shows SEM micrographs of as-spun nanofibers and calcined TiO_2/PVP composite nanofibers prepared using PVP concentrations of 7, 10, and 15 wt.%. The diameters of the as-spun TiO_2/PVP composite nanofibers increased with increasing the concentration of PVP as shown in Fig. 3(a), (b) and (c). The as-spun composite nanofibers appeared quite smooth due to the amorphous nature of TIAA/PVP composite, and each individual nanofiber was quite uniform in cross section. However, some beads were found in the as-spun TiO_2/7 wt.% PVP composite nanofibers (Fig. 3(a)). At low viscosity, polymer chain entanglements are also low and there is a higher likehood that beads fibers are obtained instead of smooth fibers [29]. The electrospun beaded fibers are

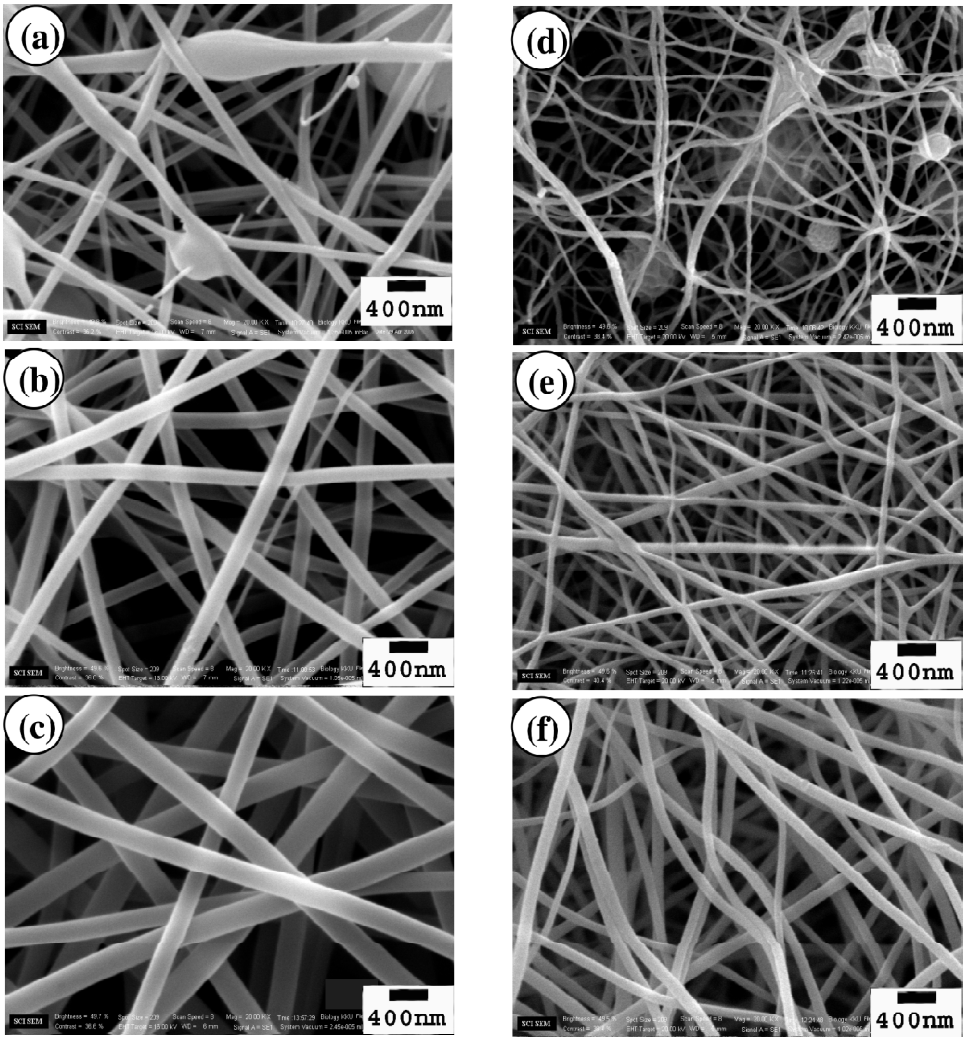

Figure 3: SEM images of the as-spun and calcined TiO_2/PVP composite nanofibers with different PVP concentrations, (a) and (d) 7 wt.% PVP, (b) and (e) 10 wt.% PVP, (c) and (f) 15 wt.% PVP. Calcination was carried out at 500 °C for 3h in air.

related to the instability of the jet of polymer solution, which has been studied by Fong *et al.* [29]. The presence of the beads in the as-spun TiO_2/7 wt.% PVP composite nanofibers is possibly due to the increasing solution instability. This is because the low viscosity of the solution resulted in the polymer and metal ions being not interacting properly.

Figure 4 shows a plot of the average diameters of the fibers as a function of PVP concentration. The diameters of the as-spun TiO_2/PVP composite nanofibres were the range of 106 ± 38 nm to 311 ± 42 nm. The PVP was selectively removed by calcinations the as-spun composite nanofibers in air at 500 °C for 3h. After calcination, the nanofibers remained as continuous structures (Figure 3(d), 3(e), and 3(f)). The diameters of the calcined nanofibers were smaller than those of the as-spun nanofibres, and the average diameters of the fibers were the range of 64 ± 15 to 127 ± 24 nm (See—Table 1). The reduction in size of the nanofibers could be attributed to the loss of PVP from the nanofibers [13,21,30] and the crystallization of TiO_2 [13,21]. It is seen that the beads still existed in the calcined 7 wt.% PVP/TiO_2 composite nanofibers (Fig. 3(d)).

Figure 5 shows the XRD results of the TiO_2/PVP composite nanofibres calcined in air at 500°C for 3h. XRD peaks of TiO_2 were detected in the range of 2θ between 20-80°. In the calcined sample of TiO_2/7 wt.% PVP composite nanofibres (Figure 5(a)), the peaks of pure anatase at 2θ as 25.4°, 37.9°, 48.2°, 54.0°, 55.2°, 62.9°, 69.0° and 75.2° corresponding to (101), (004), (200), (105), (211), (204), (116) and (215) planes were observed. The calcined samples of TiO_2/10 wt.% PVP and TiO_2/15 wt.% PVP composite nanofibers (Figure 5(b) and 5(c)) exhibited a mixture of anatase and rutile phases. The diffraction peaks of rutile at 2θ of 27.5°, 36.2°, 41.4°, and 56.8° corresponding to (110), (101), (111) and (220) planes were observed, whereas, the main peaks of anatase were also detected. It is clear that the peaks intensity of rutile(110) increased when the PVP concentration increased from 10 to 15 wt.%, corresponding to the content of rutile phase of 7 and 25 wt.% for the calcined samples of TiO_2/10 wt.% PVP and TiO_2/15 wt.% PVP composite nanofibers, respectively. The content of rutile phase presented in the samples is also tabulated in Table 1.

The formation of TiO_2 nanofibers was further monitored by Raman spectroscopy which can used to distinguish spectra of the anatase and rutile phases of TiO_2. In particular, anatase has six Raman active modes, $A_{1g} + 2B_{1g} + 3Eg$ and three infrared active modes, $A_{2u} + 2E_u$. In the case of anatase single crystal, six allowed bands in the first-order Raman spectrum were identified at 144 cm^{-1} (E_g), 197 cm^{-1} (E_g), 399 cm^{-1} (B_{1g}), 513 cm^{-1} (A_{1g}), 519 cm^{-1} (B_{1g}), and 639 cm^{-1} (Eg) [31]. Rutile has a total of 15 vibrational modes with

Table 1
Summary of the Properties and Preparation Conditions of TiO_2/PVP Composite Nanofibres Calcined in Air at 500°C for 3 h.

PVP concentration	*Crystal structure*	*Rutile content by XRD(%)*	*Fiber diameter (nm)*	*BET surface area (m^2/g)*
7	Anatase	0	64 ± 15	90
10	Anatase + Rultie	7	89 ± 22	68
15	Anatase + Rultie	25	127 ± 25	47

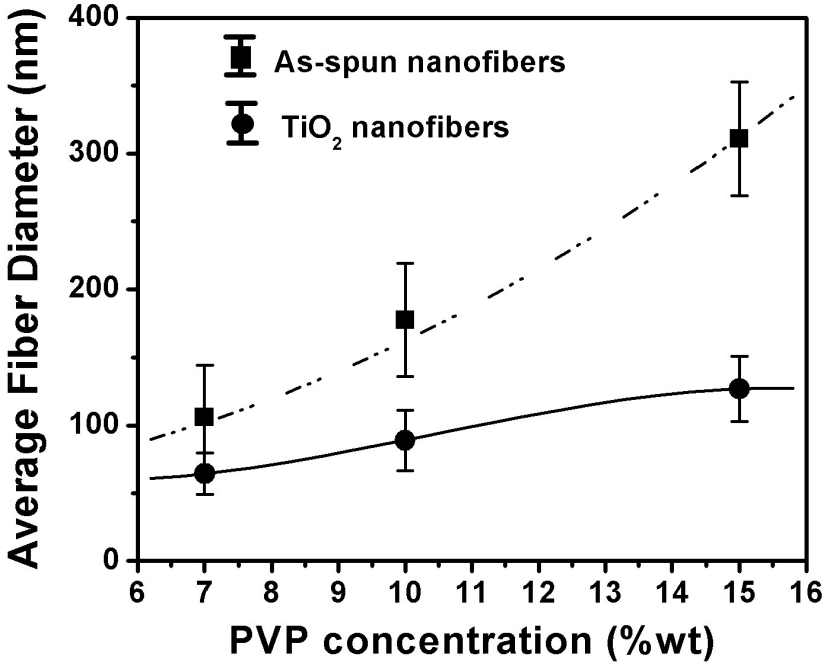

Figure 4: Average diameter of the as-spun and calcined TiO_2/PVP composite nanofibers with different PVP concentrations.

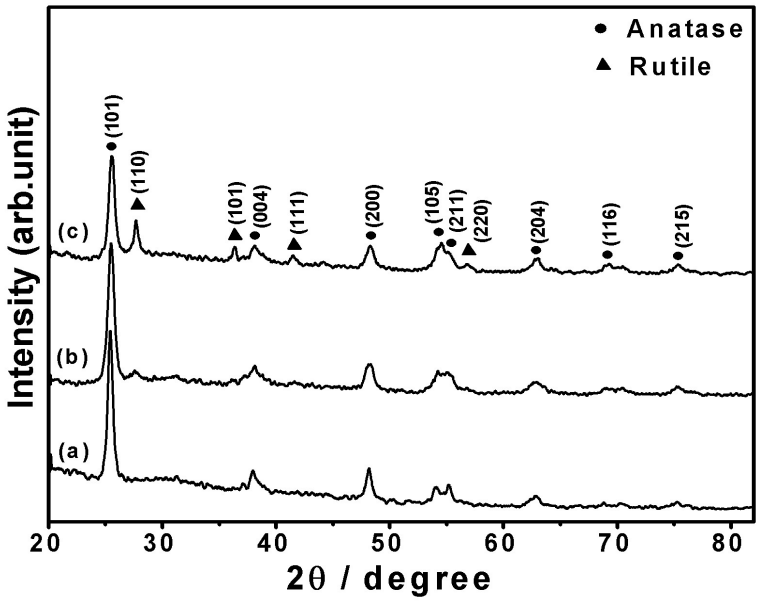

Figure 5: XRD patterns of the calcined TiO_2/PVP composite nanofibers prepared with different PVP concentrations, (a) 7 wt.% PVP, (b) 10 wt.% PVP and (c) 15 wt.% PVP.

the following irreducible representation: $A_{1g} + A_{2g} + A_{2u} + B_{1g} + B_{2g} + 2B_{1u} + E_g + 3E_u$. Among them, four modes, $A_{1g} + B_{1g} + B_{2g} + E_g$ are Raman active and four modes, $A_{2u} + 3E_u$, are infrared active. As for rutile single crystal, four Raman-active phonons were detected at 143 cm^{-1} (B_{1g}), 447 cm^{-1} (E_g), 612 cm^{-1} (A_{1g}), and 826 cm^{-1} (B_{2g}) [32]. Raman spectra of the calcined TiO_2/PVP nanofibers are shown in Figure 6(a). In all samples of the calcined TiO_2/PVP nanofibers, a strong sharp band at 144 cm^{-1}, three mid-intensity bands at 399, 519, and 639 cm^{-1} and a weak band at 197 cm^{-1} were observed. Including the superimposition of two fundamental peaks near 519 cm^{-1}, these six peaks corresponded to the six fundamental vibrational modes of anatase TiO_2 with the symmetries of E_g, E_g, B_{1g}, A_{1g}, B_{1g}, E_g, respectively [31]. Moreover, the calcined samples of TiO_2/10 wt.% PVP and TiO_2/15 wt.% PVP nanofibers showed extra two peaks at 447 and 609 cm^{-1} (Fig. 6(b)). The 447 and 609 cm^{-1} peaks are characteristic of the rutile crystal phase, suggesting that the TiO_2 nanofibers are composed of a mixture of anatase and rutile [32, 33], having anatase as the major component. In Figure 6(b), as the PVP concentration increases, the intensities of the rutile bands at 447 and 609 cm^{-1} increase, indicating an increase in the ratio of rutile to anatase. This variation of phases process is in good agreement with the XRD results. It is seen that XRD and Raman results confirm the effectiveness of PVP in promoting the anatase to rutile transformation of electrospun TiO_2 nanofibers.

The effects of PVP on phase transformation of nanocrystalline TiO_2 powders from anatase to rutile have also been investigated by Zheng *et al.* [34]. These authors found that PVP could noticeably enhance the transformation from anatase to rutile by reducing the onset transformation temperature. The transformation from anatase to rutile started at 700°C for TiO_2 powders prepared from pure TiO_2 gel without PVP [35], whereas the transformation began at 450°C and completed at 650°C for TiO_2 powders prepared from TiO_2 gel with PVP [34].

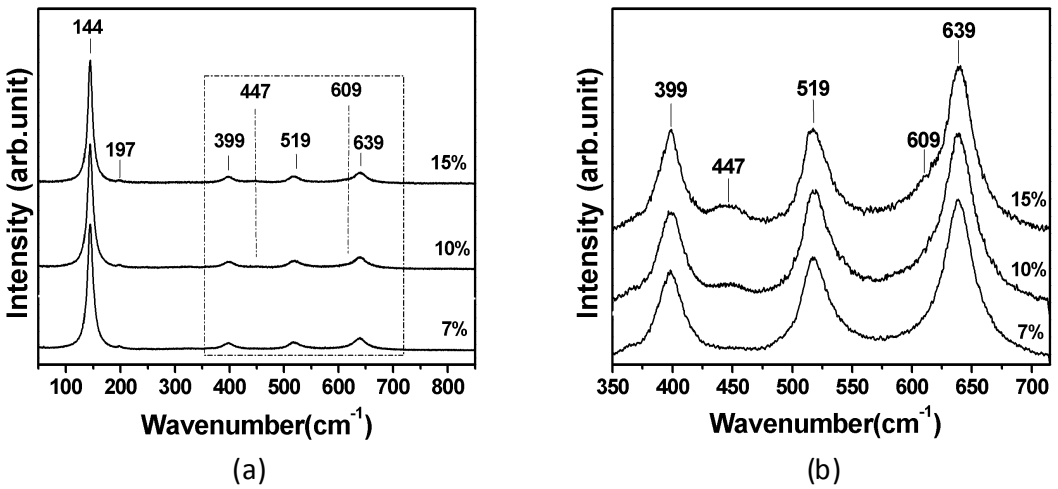

Figure 6: Raman results. (a) Raman spectra of calcined TiO_2/PVP composite nanofibers were prepared with different PVP concentrations. (b) Enlarge scale of Raman spectra in the range of 350-715 cm^{-1}

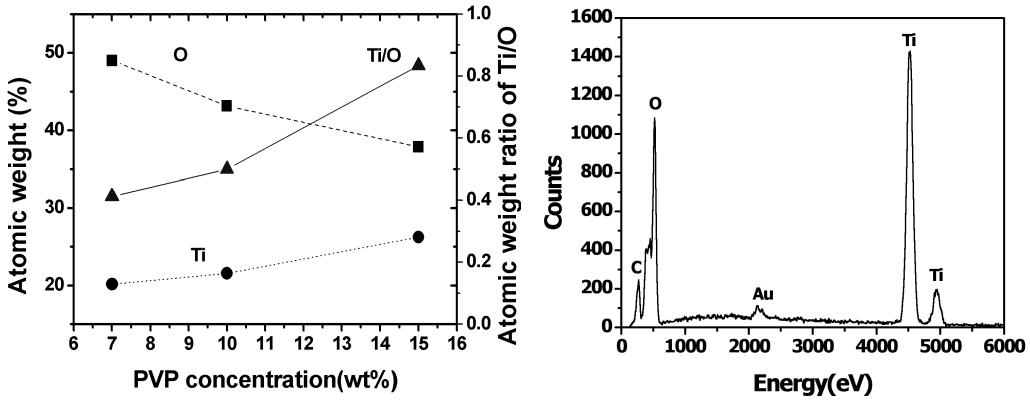

Figure 7: (a) Atomic weight and atomic weight ratio of Ti/O elements, (b) EDX spectra of TiO_2/PVP composite nanofibers (7 wt.% PVP)

Figure 7 shows the EDS results of the calcined TiO_2/PVP composite nanofibres. The atomic fraction (%) of Ti and O for the samples prepared with different PVP concentrations is shown in Fig. 7(a). When the PVP concentration increases the atomic weight (%) of Ti increases but that of O decreases. As a result, the atomic weight ratio of Ti/O increases with increasing the PVP concentration. The EDS spectrum of the sample of TiO_2/7 wt.% PVP composite nanofibers is presented in Fig. 7(b). The peaks of Ti and O were observed. The Au and C came from a gold coating and carbon film.

The BET surface areas are obtained to be 47, 68, and 90 m^2/g for the calcined samples of TiO_2/10 wt.% PVP and TiO_2/15 wt.% PVP composite nanofibres, respectively. The measured surface area is consistent with the measurements of fiber diameter. The smaller the fiber diameter, the larger the surface area. The BET surface areas of all samples are also tabulated in Table 1.

4. CONCLUSION

Electrospinning is an easy and effective technique for producing TiO_2 nanofibers with small diameters of 64-127 nm and high surface area of 47-90 m^2/g. The diameter of TiO_2 nanofibers increased with increasing PVP concentration. Beads formed in the electrospun nanofibres when the low concentration of PVP was used. The XRD and Raman results confirmed that PVP can effectively promote the anatase to rutile transformation of electrospun TiO_2 nanofibers. The effects of doping with Zr, Fe, La, and Si on anatase phase stability and photocatalytic properties of TiO_2 nanofibers are under investigation and will be reported elsewhere in the near future.

ACKNOWLEDGMENTS

The authors would like to thank the Department of Biology for providing SEM facilities, the Department of Chemistry for providing TG-DTA, the Department of Chemical Engineering for providing BET surface area measurement. This work is financially

supported by The Integrated Nanotechnology Research Center (INRC), Khon Kaen University.

References

[1] Y. Huang, X. Duan, Q. Wei and C.M. Lieber. Science, 291(2001) 630.

[2] M. H. Huang, S. Mao, H. Feick, H. Yan, Y. Wu, H. Kind, E. Weber, R. Russo and P. Yang. Science, 292(2001) 1897.

[3] Y. Xia, P. Yang, Y. Sun, Y. Wu, B. Mayers, B. Gates, Y. Yin, F. Kim and H. Yan, Adv. Mater. 15(2003) 353.

[4] J. C. Parker, R. W. Siegel, Appl. Phys. Lett. 57 (1990) 943.

[5] M. Anpo, Pure Appl. Chem. 72 (2000) 1265.

[6] M. Gratzel, M. Nature 414 (2001) 338.

[7] Z. Guan, X. Zhang, Y. Ma, Y. Cao, J. Yao, J. Mater. Res. 16 (2001) 907.

[8] A. Corma, Chem. Rev. 97 (1997) 2373.

[9] A. J. Maira, K. L. Yeung, C. Y. Lee, P. L. Yue, C. K. Chan, J. Catalysis 192 (2000) 185.

[10] P. Hoyer, Adv. Mater. 8 (1996) 857.

[11] S. J. Limmer, S. Seraji, J. Forbess, Y. Wu, P. Chou, C. Nguyen, G. Cao, Adv. Mater. 13 (2001) 1269.

[12] S. R. Mukai, H. Nishihara, S. Shichi, H. Tamon, Chem. Mater. 16 (2004) 4987.

[13] D. Li, Y. Xia, Nano Lett. 3 (2003) 555.

[14] D. Li, Y. Wang, Y. Xia, Nano Lett. 3 (2003), 3.

[15] P. Viswanathamurthi, N. Bhattarai, C. K. Kim, H. Y. Kim, D. R. Lee, Inorg. Chem. Comm. 7 (2004) 679.

[16] S. Madhugiri, B. Sun, P. G. Smirniotis, J. P. Ferraris, K. J. Balkus Jr., Micropor. Mesopor. 69 (2004) 77.

[17] J. T. MaCann, D. Li, Y. Xia, J. Mater. Chem. 15 (2005) 735.

[18] S. H. Lee, C. Tekmen, W. M. Sigmund, Mater. Sci. Eng. A 398 (2005) 77.

[19] M. Y. Song, D. K. Kim, K. J. Ihn, S. M. Jo, D. Y. Kim, Synthetic Metals 153 (2005) 77.

[20] W. K. Son, D. Cho, W. H. Park, Nanotechnology 17 (2006) 439.

[21] W. Nuansing, S. Nilmuang, W. Chareonboon, S. Maernsiri and S. Seraphin, Mater. Sci. Eng. B 131 (2006) 147-155,

[22] D. H. Renaker, I. Chun, Nanotechnology 7 (1996) 216.

[23] A. Frenot, I. S. Chronakis, Curr. Opin. Colloid. Inter. Sci. 8 (2003) 64.

[24] Z. H. Huang, Y. Z. Zhang, M. Kotaki, S. Ramakrishna, Comp. Sci. Tech. 63, 2003, 2223.

[25] D. Li, Y. Xia, Adv. Mater. 16 (2004) 1151.

[26] W. Sigmund, J. Yuh, H. Park, V. Maneeratana, G. Pyrgiotakis, A. Daga, J. Taylor, J. C. Nino, J. Amer. Ceram. Soc. 89 (2006) 395.

[27] J.A. Gamboa, D.M. Pasquevich, J. Am. Ceram. Soc. 75 (1992) 2934.

[28] R.A. Spurr, H. Myers, Anal. Chem. 29 (1957) 760.

[29] H. Fong, I. Chun, D.H. Reneker, Polymer. 40(1999) 4585.

[30] S. Maensiri, W. Nuansing, J. Klinkaewnarong, P. Laokul, J. Khemprasit, J. Colloid Interface Sci. 297 (2006) 578.

[31] T. Ohaka, J. Phys. Soc. Jpn. 48 (1980) 1661.

[32] S. P. S. Porto, P. A. Fluery, T. C. Damen, Phys. Rev. 154 (1967) 522.

[33] Y. H. Zhang, C. K. Chan, J. F. Porter and W. Guo, J. Mater. Res. 13 (1998) 2602.

[34] M. P. Zheng, M. Y. Gu, Y. P. Jin, H. H. Wang, P. F. Zu, P. Tao, J. B. He, Mater. Sci. Eng. B 87 (2001) 197.

[35] M. P. Zheng, M. Y. Gu, Y. P. Jin, Acta Mater. Sin. 35 (1999) 1224.